

Angular distributions of suprathermal electrons observed at geosynchronous orbit

M. O. Fillingim,¹ M. B. Moldwin, H. K. Rassoul, and P. Parrish

Department of Physics and Space Sciences, Florida Institute of Technology, Melbourne

M. F. Thomsen and D. J. McComas

Space and Atmospheric Science Group, Los Alamos National Laboratory, Los Alamos, New Mexico

Abstract. Six months of low-energy electron plasma data collected using the Los Alamos National Laboratory magnetospheric plasma analyzer (MPA) onboard the geosynchronous satellite 1989-046 have been surveyed. The MPA instrument measures the three-dimensional energy per unit charge distributions of cold ions and electrons, allowing for the simultaneous determination of the angular distribution and ambient plasma regime. Suprathermal electrons in the energy range 15 to 200 eV were characterized by local time of occurrence, angular distribution, and ambient plasma regime. Results indicate a local time dependence in angular distributions, with trapped distributions, i.e., enhanced fluxes of particles with pitch angles near 90° and 270°, primarily being observed in the morning, coincident trapped and field-aligned angular distributions (enhanced fluxes of particles with pitch angles near 90° and 270° coincident with enhanced fluxes of particles with pitch angles near 0° and 180°) occurring around noon, a lack of detectable low-energy electron fluxes near dusk, and a complex combination of angular distributions on the nightside. When both trapped and field-aligned angular distributions are present, the field-aligned component generally has lower energy than the trapped component. Dayside field-aligned angular distributions are interpreted as being photoelectrons from the ionosphere, while trapped angular distributions are from the low-energy tail of the plasma sheet distribution. A plasma regime dependence in angular distributions was also observed. Plasma sheet angular distributions are generally isotropic or trapped. The plasma trough angular distributions are trapped or coincident trapped and field-aligned. Plasmaspheric electrons commonly have energies below our 15 eV threshold.

1. Introduction

1.1. Plasma Regimes Observed at Geosynchronous Orbit

Geosynchronous orbit is unusual in that at this altitude a spacecraft may enter into many different plasma regimes depending upon local time and geomagnetic activity. In the dusk sector, a spacecraft often encounters the dusk bulge of the outer plasmasphere during a typical orbit [Carpenter, 1966; Chappell *et al.*, 1970; Higel and Wu, 1984]. This region is characterized by relatively dense ($\sim 10\text{--}100\text{ cm}^{-3}$ at synchronous orbit),

low-energy ($\sim 1\text{ eV}$), isotropic plasma [Moldwin *et al.*, 1994].

After exiting the plasmasphere, the spacecraft almost immediately enters the plasma sheet, characterized by less dense ($\sim 1\text{ cm}^{-3}$), higher-energy ($\sim 1\text{ keV}$), electrons [Horwitz *et al.*, 1986; McIlwain and Whipple, 1986; McComas *et al.*, 1993]. Plasma sheet electrons are typically seen in the night/dawn sector at geosynchronous orbit.

On the dayside, as the energy density of the electrons slowly decreases, the spacecraft enters the plasma trough [Carpenter, 1966; Wrenn *et al.*, 1979; Thomsen *et al.*, 1998]. The dayside plasma trough is characterized by warm ($\sim 10\text{ eV}$), field-aligned fluxes of ions from the ionosphere [Sojka *et al.*, 1983; Wrenn *et al.*, 1983]. It is supposed that these plasma trough fluxes are the source of plasmaspheric refilling.

During periods of quiet geomagnetic activity, the plasmasphere expands and can be seen at all local times at geosynchronous orbit [Sojka and Wrenn, 1985; Mold-

¹Now at Geophysics Program, University of Washington, Seattle.

wm et al., 1994]. During intervals of high geomagnetic activity, the conditions at geosynchronous orbit change dramatically. The inner edge of the plasma sheet convects earthward as geomagnetic activity increases [*Vasyliunas*, 1968]. The increase in the convection electric field which causes this migration also strips away the outer regions of the plasmasphere. The plasmaspheric dusk bulge generally does not disappear at geosynchronous orbit but moves to earlier local times (toward noon) and has a smaller extent [*Higel and Wu*, 1984; *Moldwin et al.*, 1995]. Extreme geomagnetic activity may move the tail lobe or the low latitude boundary layer (LLBL) to geosynchronous altitudes [*McComas et al.*, 1993].

For a more detailed description of the different plasma regimes seen at geosynchronous orbit, see *McIlwain and Whipple* [1986] or *McComas et al.* [1993]. Example energy spectrograms of the different plasma environments observed at geosynchronous orbit during the period of this study will be discussed in the Methodology section.

1.2. Suprathermal Electrons at Geosynchronous Orbit

Suprathermal electrons (energies of a few hundred eV and lower) play an important role in heating the thermal ionospheric and plasmaspheric plasma and contribute to optical emissions and ionization of the upper atmosphere [*Liemohn and Khazanov*, 1995]. Also, in the presence of hot plasma, suprathermal electrons have important influences on instability conditions that can produce electrostatic electron cyclotron waves [*Fairfield and Viñas*, 1984].

Using the suprathermal plasma analyzers (SPA) onboard the geosynchronous satellite GEOS 2, *Wrenn et al.* [1979] examined the low-energy electron populations in the morning and day sectors. These instruments measured trapped (pitch angles ~ 90 deg; also called “pancake” distributions) electrons in the energy range of 50 to 500 eV in the morning sector at geosynchronous orbit. The SPA could detect electron energies down to ~ 1 eV; however, the lowest energies were contaminated by local photoemission from the satellite spacecraft surfaces. For this reason, only electrons with energies greater than 50 eV were examined in their study. *Wrenn et al.* [1979] suggested that the trapped distributions may have been due to wave particle interactions created when cold plasma from the ionosphere mixed with the hot plasma sheet and ring current particles. Later, the authors also proposed that these warm, trapped electrons could have been the remnants of plasma sheet particles which had $\mathbf{E} \times \mathbf{B}$ drifted from the nightside to the dayside [*Sojka and Wrenn*, 1985].

Garrett et al. [1981] performed a large-scale statistical study of low-energy electrons measured at geosynchronous orbit using data from ATS 5 and ATS 6. They found that the electron distribution functions were not simple Maxwellian distributions. The data were better

described by a two component distribution: one relatively cool (~ 100 to ~ 1000 eV), and the other hot (~ 10 to ~ 100 keV). The number density of the cool component averaged about 1 cm^{-3} with a slight minimum in the afternoon. Also, the temperature of the cool component was greatest near local midnight and gradually decreased in the morning sector. Probable sources of the lower-energy particles were suggested to be either residual low-energy plasma left over following injection events or the high-energy tail of the plasmaspheric plasma.

Fairfield and Viñas [1984] also presented evidence for a cool electron component in close proximity to the near-Earth plasma sheet boundary using the ISEE 1 low energy spectrometer. Their observed rise in the electron energy spectrum accompanying the spacecraft’s entrance into the inner edge of the plasma sheet was consistent with the earlier observations of *Vasyliunas* [1968]. This rise in electron energy spectrum was explained as a result of energy-dependent magnetic drifts. Because of magnetic gradient-curvature drifts, less energetic particles are able to penetrate closer to Earth before drifting eastward (in the case of electrons) forming an inner boundary. On the night side, as the spacecraft crossed into the plasma sheet, *Fairfield and Viñas* [1984] reported a decrease in the flux of particles with 90° pitch angles with energies corresponding to the energy boundary being crossed. Well inside the plasma sheet, particle distributions were isotropic; however, as the spacecraft approached the morning sector, an enhancement of particle fluxes near 90° pitch angle was observed. These observations were shown to be consistent with single particle simulations [e.g., *Cowley and Ashour-Abdalla*, 1975].

Coates et al. [1985] used the suprathermal plasma analyzers on both GEOS 1 and GEOS 2 spacecrafts to measure low-energy (< 100 eV) field-aligned electron fluxes on the dayside. *Coates et al.* [1985] compared these field-aligned electron fluxes with ionospheric photoelectron fluxes measured by *Lee et al.* [1980] using the Atmospheric Explorer (AE) satellite at an altitude of 350 km. *Coates et al.* [1985] found that the energy spectrum of the low-energy field-aligned fluxes matched well with the ionospheric photoelectron energy spectrum. They also observed that these low-energy electron field-aligned fluxes “turned on” at dawn as the conjugate ionospheres became sunlit. It was concluded that field-aligned flows of electrons below 100 eV observed at geosynchronous orbit were photoelectrons from the ionosphere.

Presented in the following sections is a long-term survey of 15 to 200 eV electrons observed at geosynchronous orbit. Section 2 will describe the instrument and show an example of a typical energy spectrogram surveyed in this study. The angular distribution of 15 to 200 eV electrons as a function of local time for a large sample will be shown in section 3. Another key result, the dependence of the angular distribution of 15

to 200 eV electrons on the ambient plasma regime, will be illustrated in section 4. Section 5 will discuss the conclusions and summarize the results of this study.

2. Methodology

2.1. Instrument

Plasma observations obtained from the Los Alamos National Laboratory's magnetospheric plasma analyzer (MPA) on board the geosynchronous spacecraft 1989-046 over the interval from September 1991 through July 1992 were surveyed for this study. The instrument is composed of a spherical section electrostatic analyzer followed by six independent channel electron multipliers (CEMs) which view six different ranges of polar angle relative to the spacecraft spin axis. The spacecraft spins about an axis continuously pointed at Earth and completes one revolution every 10 s. The MPA field of view is oriented normal to the spacecraft spin axis and covers the polar angle range of $\pm 66^\circ$. In this way, nearly 92% of 4π steradians are sampled during each 10-s spin. The energy range of the detector is nominally ~ 1 eV/q to ~ 40 keV/q for both ions and electrons, and a full three-dimensional distribution for one species is obtained in one spin of the spacecraft. During the normal mode of operation, one full three dimensional electron distribution function and two full 3-D ion distribution functions are measured every 86 s. For a comprehensive description of the MPA instrument, see *Bame et al.* [1993] or *McComas et al.* [1993].

During the time interval of this study, satellite 1989-046 was located at 195 deg east longitude, or equivalently, the local time of the spacecraft was 11 hours behind universal time. One instrument lacking on this spacecraft is a magnetometer. It is for this reason that the pitch angle distributions of the particles are not measured; only the azimuthal angular distribution normal to the satellite-Earth line is measured. However, the spacecraft nominally remains within a few degrees of the magnetic equator throughout its orbit. Since the spacecraft is spin stabilized with its spin axis pointing towards Earth and orbits within a few degrees of the magnetic equator, the field-aligned direction is assumed to be directly north south, perpendicular to both the path of the spacecraft's orbit and its spin axis [cf. *Thomsen et al.*, 1996]. At times, especially during periods of high magnetic activity, Earth's magnetic field at geosynchronous orbit may be significantly distorted from a true dipole, so this assumption may not be strictly valid. On average, however, this is a reasonable assumption.

A sun shade is present on the instrument that prevents direct solar radiation from entering the aperture. However, the sun shade does not completely prevent the corruption of electron data at some limited spin angles as a result of solar illumination. Photoemission from the shield and instrument surfaces results in a charac-

teristic solar radiation signature in the energy spectrograms present at all local times. The contamination due to locally produced photoelectrons covers the lowest 10 eV and is approximately 40° wide in azimuthal angle on the electron energy spectrogram as shown in the bottom panel of Plate 1. The position of the contamination varies in angle with local time and season. Because of this persistent feature, this study is confined to electrons with energies greater than 15 eV.

While immersed in the hot electron plasma sheet, the satellite can acquire a large negative potential, up to and sometimes exceeding several hundred volts. This negative potential attracts and accelerates nearby low-energy ions yielding characteristic step-like features such as those present in the ion energy spectrogram (second panel from the bottom in Plate 1) between 1100 and 1900 UT (0000 to 0800 LT) on July 24, 1992, and between 1100 and 1900 UT (0000 to 0800 LT) on July 25, 1992. Large negative potentials also repel low-energy electrons, giving a false indication of reduced low-energy electron fluxes. Spacecraft charging can account for the lack of low-energy electron fluxes between 1100 and 1500 UT (0000 and 0400 LT) July 24, 1992, and between 1100 and 1600 UT (0000 and 0500 LT) July 25, 1992.

2.2. Data Set

Six months of plasma data were included in this survey: September 1991, December 1991, February 1992, March 1992, June 1992, and July 1992. These months were chosen in an attempt to cover the equinoxes, solstices, and representative months in between. The low-energy (15 to 200 eV) electron angular distribution and ambient plasma regime were recorded for every half-hour local time interval for a total of 48 local time bins per day. The data used to determine azimuthal angle were binned into 18 equally spaced angular bins, for an effective azimuthal angle resolution of 20° (as it appears in the color energy spectrogram of Plate 1).

Energy fluxes with peaks at least 30% above the background flux centered between 45° and 135° and between 225° and 315° were termed "trapped." Electron fluxes with peaks between 315° and 45° and between 135° and 225° were termed "field-aligned." If there were no peaks 30% higher than surrounding fluxes, the distribution was termed "isotropic." For peaks in both the trapped and field-aligned regimes with substantial ($\sim 30\%$) gaps in electron flux between them, the distribution was termed "both" or "trapped/field-aligned." When no detectable electron fluxes were present in the 15 to 200 eV range, the distribution was termed "none." A sixth category was made for angular distributions which did not meet any of these criteria termed "other." For half-hour local time bins which contained more than one angular distribution, the angular distribution occurring for the longest amount of time within the half-hour interval was chosen to represent to entire interval.

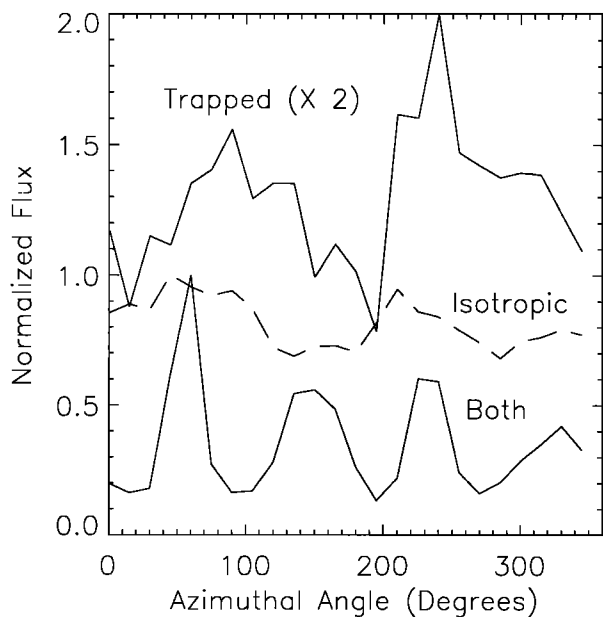


Figure 1. Normalized flux of low-energy (15 to 200 eV) electrons versus azimuthal angle for selected distributions. All of these distributions were measured on July 24, 1992. The “both” (trapped/field-aligned) distribution was measured at 0200 UT; the “isotropic” distribution at 1000 UT; and the “trapped” at 1530 UT. The “trapped” distribution has been multiplied by 2 for clarity.

Figure 1 shows line plots of flux versus azimuthal angle illustrating trapped ($\times 2$ for clarity), isotropic, and both distributions.

The determination of angular distribution was done by eye and, as such, are inherently subjective. Quantitative criteria were employed in an attempt to minimize subjectivity. The criteria used to determine the plasma regime was similar to those used by *McComas et al.* [1993] and will be more completely discussed in the next section.

Approximately 85%, nearly 7500 data points, of the total data set was usable for the purpose of determining angular distribution-local time relationships; the remaining 15% consisted of data gaps. The first row of Table 1 shows the percentage of data that was used to determine the angular distribution versus local time relationships for each month and for the entire data set.

Over 6000 data points, 70% of the total data set, were used to relate angular distribution to plasma regime. The additional 15% of the plasma data was not used

because of high background contamination of ion fluxes. High background contamination, which consisted of apparent low fluxes of ions at all azimuthal angles and at all energies, prevented the unambiguous determination of plasma regime. It is thought that this contamination was due to direct penetration of the detectors by highly energetic protons from solar energetic particle events or by relativistic electrons of the outer radiation belt. The second row of Table 1 tabulates the percent of usable data for relating angular distribution to plasma regime. The percent of usable data is shown for all six months as well as for the entire data set. High background contamination was encountered during the months of September 1991, December 1991, and March 1992; the remaining months were not significantly affected.

For the purposes of this study, spacecraft charging intervals, as described in the previous section, were not removed. A survey of these intervals indicates that spacecraft charging occurs in the plasma sheet, usually between 0000 and 0600 LT. The effect of spacecraft charging on the low-energy electron distribution is to decrease the flux to low or undetectable levels. Typically, during intervals of spacecraft charging, negligible low-energy electron fluxes are measured, i.e., the angular distribution recorded during spacecraft charging intervals is usually “none.”

2.3. Typical Spectrogram

Plate 1 is an example energy spectrogram containing 2 days of data from July 24 and 25, 1992. This representative interval was chosen because it contains each of the plasma regimes commonly observed at geosynchronous orbit. The angular distributions observed during this time also agree well with the average trends which result from surveying 6 months of data.

The horizontal axis begins at 0000 UT (1300 LT) on July 24, 1992, and spans two complete days. The bottom panel plots the color coded logarithm of the electron count rate as a function of the logarithm of the energy of the electrons versus time; the next panel up shows the same for the ions. The two uppermost spectrograms show the azimuthal angle distribution of the electrons in two different energy ranges versus time. The top panel shows the distribution of electrons in the 15 to 200 eV energy range, the range studied for this survey. The second panel shows the distribution in the 3 to 44 keV energy range for comparison only.

The count rates are proportional to the energy flux and are scaled to the color bar through the “min” and

Table 1. Percentages of Data Usable for Determining Angular Distribution Relationships

AD Relationship	Sept. '91	Dec. '91	Feb. '92	March '92	June '92	July '92	All Months
AD-LT	86%	75%	93%	88%	82%	83%	85%
AD-plasma regime	53%	39%	93%	68%	82%	83%	70%

“max” numbers for each spectrogram. For example, consider the electron energy spectrogram (bottom). A red flux in this spectrogram corresponds to a count rate of $10^{3.0}$ particles per 0.009-s counting interval, or about 10^5 s^{-1} . A green flux (midrange) corresponds to $10^{1.5}$ particles per 0.009-s interval, or $\sim 3500 \text{ s}^{-1}$.

One apparent feature in the bottom spectrogram is the contamination due to photoemission produced locally at the spacecraft in the lowest 10 eV energy range at all local times. Because of this persistent feature, this study is confined to electrons with energies greater than 15 eV. Additionally, energetic ions ($> \sim 10 \text{ keV}$) can be seen at all local times in the ion spectrogram; this energetic ion component is the low-energy tail of the ring current.

Following the categorization scheme of *McComas et al.* [1993], plasmaspheric regions are characterized by intense fluxes (yellow or higher, which corresponds to $> \sim 3500 \text{ s}^{-1}$) of ions having energies lower than 10 eV. This flux corresponds to a low-energy ion number density of $> \sim 10 \text{ cm}^{-3}$ [*Moldwin et al.*, 1995]. Plasmaspheric regions are seen between approximately 0400 and 0830 UT (1700 and 2130 LT) on July 24, and between 0730 and 0830 UT (2030 and 2130 LT) on July 25.

Plasma sheet populations are characterized by intense fluxes (yellow or higher, which corresponds to $> \sim 7000 \text{ s}^{-1}$) of electrons with energies greater than 1 keV. These criteria are met for the time intervals between 1000 and 2000 UT (2300 and 0900 LT) on July 24, and shortly after 0800 UT (2100 LT) until 1900 UT (0800 LT) on July 25. However, after these times an appreciable flux of energetic plasma sheet-like electrons persist. (The transition from plasma sheet to electron trough is gradual, and the specific transition point is somewhat arbitrary [*Thomsen et al.*, 1998], but we maintain the distinction for consistency with previous work.) As discussed earlier, spacecraft charging intervals are seen in the plasma sheet between 1100 and 1900 UT (0000 and 0800 LT) July 24, and between 1100 and 1900 UT (0000 and 0800 LT) July 25.

Regions of plasma trough, characterized by low fluxes of warm ($\sim 10 \text{ eV}$) ions, were present between the beginning of July 24 until 0400 UT (1700 LT). The time interval between exiting the plasma sheet at 2000 UT (0900 LT) and entering the plasmasphere at 0730 UT (2030 LT) on July 25 is classified as plasma trough (excluding data gaps) even though the most intense warm ion fluxes occur only between 1000 and 1600 LT. For the purposes of this study, no distinction is made between the refilling trough (as seen here) and the empty trough (devoid of both low-energy ion fluxes and high-energy electron fluxes) as separately categorized by *McComas et al.* [1993]. Again, plasma trough signatures are seen from the exiting of the plasma sheet at 1900 UT (0800 LT) on July 25 to the end of the spectrogram.

Coincident trapped and field-aligned angular distributions, whose criteria were discussed in the Data Set section, are present in the 15 to 200 eV energy range

from the beginning of the spectrogram until 0530 UT (1830 LT), when the angular distribution changes to field-aligned. (The slight east-west imbalance (imbalance between the 90° and 270° azimuthal angle fluxes) in the flux of low-energy electrons between 0530 and 0830 UT (1830 and 2130 LT) on July 24 is most likely due to the high energy end of the locally produced photoelectrons; the Sun was to the west of the spacecraft in this sector, and thus more photoelectrons were visible in the westward looking direction. Therefore the six half-hour time bins in this interval were classified as “field-aligned.”) Trapped and field-aligned angular distributions are again present from 1900 UT (0800 LT) on July 24 to 0300 UT (1800 LT) on July 25 when the field-aligned component fades into the background leaving a trapped angular distribution until the data gaps at 0700 UT (2000 LT) on July 25. Exclusively trapped angular distributions are also seen from 1400 to 1800 UT (0300 to 0700 LT) on July 24, and again from near 1800 UT (0700 LT) on July 25 until the end of the spectrogram.

Periods of isotropic angular distributions are mostly confined to 1000 to 1100 UT (2300 to 0000 LT) on July 24, 0900 to 1100 UT (2200 to 0000 LT) on July 25, and 1700 to 1800 UT (0600 to 0700 LT) on July 25. Finally, no significant fluxes of low-energy electrons are measured between 1100 and 1500 UT (0000 and 0400 LT) July 24 and between 1100 and 1600 UT (0000 and 0500 LT) July 25 due to spacecraft charging.

3. Angular Distributions Versus Local Time

Plate 2 shows the results of our survey of low-energy electron angular distributions for the six months of data. The different colored lines show the percentage of observations in each half-hour local time bin that could be characterized according to the indicated labels. Plate 2 shows that near dawn, trapped distributions are dominant. Shortly after dawn, field-aligned distributions begin to appear in conjunction with the trapped distributions. By late afternoon there appears to be few electrons in this energy range, so “None” is the dominant category. The pre-midnight distributions are typically isotropic. Purely field-aligned distributions are relatively uncommon, but show up most often in the afternoon and evening quadrants.

Figure 2 was created by adding the trapped and trapped/field-aligned angular distribution together to get the total percentage of trapped particle occurrences versus local time. Similarly, in order to get the total percentage of field-aligned particle occurrences versus local time, the field-aligned and trapped/field-aligned angular distributions were added together. The peak of the trapped particle occurrences in the 15 to 200 eV energy range is in the morning sector, between 0800 and 0900 LT. This is in general agreement with the observations of trapped low-energy electrons in the morning

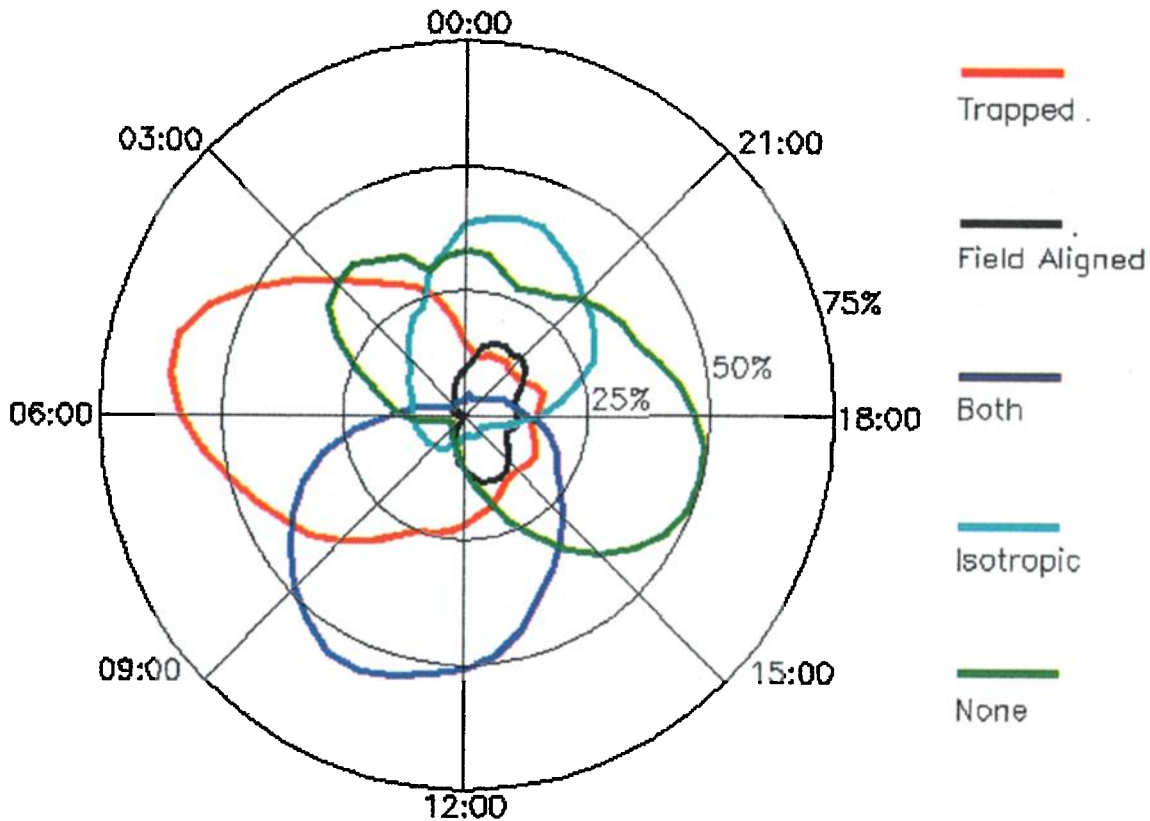


Plate 2. The local time distributions of the various low-energy electron angular distributions observed at geosynchronous orbit.

sector by *Wrenn et al.* [1979] and *Fairfield and Viñas* [1984].

The peak field-aligned particle occurrences is centered about local noon in accordance with the determination made by *Coates et al.* [1985] that low-energy field-aligned fluxes observed on the dayside are photoelectrons from the ionosphere. The field-aligned particle occurrences are also fairly symmetric on either side of noon except for the few hours before and after midnight. *Garrett et al.* [1981] noticed a similar pre-midnight/postmidnight asymmetry in the number densities of the lower-energy electrons.

4. Angular Distributions Versus Plasma Regime

Table 2 and Table 3 display the relationships between angular distribution and plasma regime. Table 2 shows the percentage of data points for the entire sample in which the particular angular distributions were observed in each plasma regime. The angular distribution percentages in each plasma regime (i.e., each column) add to approximately 100%. The columns do not add to exactly 100% due to the exclusion of "other" angular distributions and also because observations of coincident trapped and field-aligned distributions were added to both the trapped and the field-aligned per-

centages. Only the three major geosynchronous plasma regimes are included: plasma sheet, plasma trough, and plasmasphere. Occurrences of plasma sheet and plasma trough overlapping [*McComas et al.*, 1993] are ignored since this accounts for less than 10% of the usable data. Also, regions classified as "other" (e.g., tail lobe and LLBL) are not included because they make up less than 1% of the data.

In the plasma sheet, trapped fluxes of low-energy electrons are encountered nearly one third of the time. Isotropic distributions are the second most common angular distribution observed in the plasma sheet (over one fourth of the usable data points in the plasma sheet). When the spacecraft is in the plasma trough, trapped distributions are observed almost two thirds of the time. Field-aligned distributions are observed in over one third of the usable data points in this plasma regime. Finally, in nearly 85% of the observations in the plasmasphere, no fluxes of low-energy electrons in the 15 to 200 eV energy range are detected. When low-energy fluxes in this energy range are detected in plasmaspheric regions, the particles are typically field-aligned. Field-aligned low-energy electron fluxes account for ~10% of all plasmaspheric observations.

Table 3 shows the percentage of observations of each plasma regime for the specific angular distributions. Again, each column adds to approximately 100%. Col-

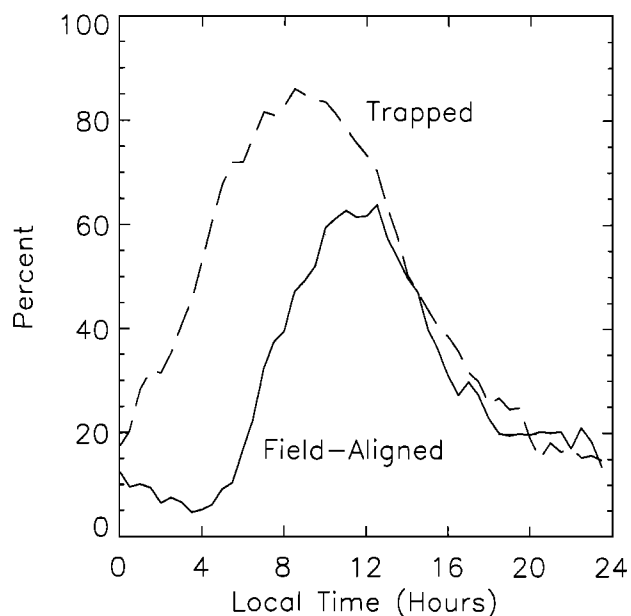


Figure 2. Percentage of valid data in each half-hour time bin that can be characterized as trapped or field-aligned. Totals can exceed 100% because many distributions exhibit both trapped and field-aligned characteristics.

umn totals are slightly less than 100% because regions of plasma sheet and plasma trough overlap have been excluded as well as “other” plasma regimes.

Over 60% of the trapped distributions are observed when the spacecraft is in the plasma trough. Almost 30% of these observations are made in the plasma sheet. Field-aligned distributions are seen most often in the plasma trough; one fourth of the field-aligned distributions are observed in the plasma sheet. When the spacecraft encounters isotropic distributions, it is usually in the plasma sheet. Isotropic distributions are observed in the plasma trough almost one fourth of the time. Slightly more instances of no detectable low-energy electron fluxes occur in the plasma sheet than in the plasmasphere. A significant fraction of no detectable electrons fluxes occur in the plasma trough, also.

5. Summary and Conclusions

By using a large, long-term data set, we found an azimuthal angle distribution versus local time relationship for electrons in the energy range 15 to 200 eV observed at geosynchronous orbit. These relationships had been explored before for specific local time intervals (e.g., *Wrenn et al.* [1979] in the morning sector, and *Coates et al.* [1985] on the dayside), but this survey also has the advantage of detecting the three-dimensional energy distribution of both low-energy ions and electrons, allowing us to associate angular distributions with plasma regime.

In the morning sector, trapped distributions are commonly observed in the 15 to 200 eV energy range, in agreement with *Wrenn et al.* [1979]. As the day progresses, a field-aligned component appears in the low-energy electron flux which is interpreted as ionospheric photoelectrons first detected by *Coates et al.* [1985] at geosynchronous orbit. On the dayside when trapped and field-aligned distributions are seen simultaneously (Plate 1, 0800 to 1900 LT), the higher-energy electrons typically also have trapped angular distributions. By comparing the two electron energy bins in Plate 1, it is apparent that when the lower-energy electrons have trapped distributions, the higher-energy electrons are also trapped. This suggests that the trapped electrons in the 15 to 200 eV energy range may be the low-energy tail of the plasma sheet which has $\mathbf{E} \times \mathbf{B}$ drifted from the nightside to the morning and day sectors.

Electron energy fluxes in the dusk bulge of the plasmasphere are too cold to be detected in this energy range. Thus our study commonly finds no detectable low-energy electron fluxes near dusk.

In the premidnight sector, an increase in isotropic low-energy electron fluxes is encountered as the spacecraft enters the near-Earth plasma sheet. In the few hours after midnight, a complex combination of angular distributions are observed, most likely due to the effects of spacecraft charging.

It is unknown at the present if the premidnight/post-midnight asymmetry observed in the low-energy field-aligned occurrences shown in Figure 2 is an instrument artifact of if it is physical. The decreasing fraction of occurrences of field-aligned electron fluxes in the postmidnight sector may be due to spacecraft charging. Typically, the signatures of spacecraft charging are seen after midnight, after the spacecraft has entered into the near-Earth plasma sheet. The increased negative potential on the spacecraft may repel these low-energy negatively charged particles. No corresponding decrease is found in the trapped low-energy electron distributions possibly because these trapped particles are the low-energy tail of the plasma sheet population. A large negative spacecraft potential will retard energetic plasma sheet particles just enough so that they can be detected in this lower-energy channel.

Alternately, there may be a geophysical explanation for the decrease in the low-energy field-aligned electron occurrences. After dusk, there is a sharp decrease in the field-aligned flux because photoelectron production by photoionization ceases. The field-aligned electron flux does not go to zero on the nightside, however, because of the drift motion of flux tubes from the day and dusk sectors due to the $\mathbf{E} \times \mathbf{B}$ drift in the presence of the corotation and convection electric fields and the magnetic gradient-curvature drifts [*Khazanov et al.*, 1996]. Continuing toward dawn, the field-aligned electron fluxes may decrease as particles are pitch angle scattered or lost to the atmosphere.

Table 3. Percentage of Observations of Each Plasma Regime for the Specific Angular Distributions

Plasma Regime	Trapped	Field-Aligned	Isotropic	None
Plasma sheet	28%	26%	65%	39%
Plasma trough	61%	65%	23%	25%
Plasmasphere	2%	5%	1%	34%

Additionally, a definite angular distribution versus plasma regime relationship was found. Our results show that the electron angular distributions is influenced, if not determined, by plasma regime. In the plasma sheet, the two most commonly observed angular distributions are trapped and isotropic distributions. This agrees qualitatively with the angular distribution-local time relationships and with plasma regime-local time relationships determined by *McComas et al.* [1993]. On average, the spacecraft enters into the near-Earth plasma sheet in the pre-midnight sector when isotropic low-energy electrons are observed. A majority of the isotropic distribution intervals occur in the plasma sheet (Table 3), and these intervals occur around local midnight (Plate 2).

Fairfield and Viñas [1984] noted that upon crossing the inner boundary of the plasma sheet, the energetic electron energy distributions corresponding to the energy boundaries being crossed were depleted near 90° pitch angle; further into the plasma sheet, the angular distributions became more isotropic. Therefore, in a study like this, one may expect to see field-aligned fluxes as the spacecraft crosses the inner boundary of the plasma sheet. However, such an effect is not seen in the low-energy electron distributions. In this study we have looked at the pitch angles of all of the electrons between 15 and 200 eV. A field-aligned enhancement at the 200 eV boundary would be drowned out by isotropic distributions at all energies below 200 eV. Additionally, field-aligned enhancements at the lowest-energy boundaries may be missed due to low fluxes of particles at these energies or the small spatial scale of the low-energy boundaries. It will be noted, however, that around 1100 UT (local midnight) on July 24, the high-energy electrons (3 to 44 keV) appear to have enhanced field-aligned fluxes for several minutes corresponding to the spacecraft's entrance into the plasma sheet.

As the spacecraft moves into the morning side and the peak energy of the near-Earth plasma sheet slowly

moves to lower energies [*Vasyliunas*, 1968], the dominant angular distribution of the low-energy electrons becomes trapped. This is consistent with previous observations. There is a significant fraction of intervals in the plasma sheet in which no detectable low-energy electron fluxes are observed. This is attributed to spacecraft charging.

Trapped and field-aligned distributions are frequently found in the plasma trough. Also, a majority of the intervals in which either trapped or field-aligned distributions are observed, the spacecraft is in the plasma trough. Constructing a table identical to Table 3 except that occurrences of coincident trapped and field-aligned distributions are not added to both the trapped distributions and field-aligned distribution occurrences but left as a separate column, we find that 75% of the intervals in which coincident trapped and field-aligned distributions are observed, the spacecraft is in the plasma trough.

However, we also note that occurrences of trapped distributions in the plasma trough are substantially higher than occurrences of field-aligned distributions. The high occurrence of exclusively trapped particles in the plasma trough is most likely due to the low-energy tail of the plasma sheet electrons drifting into the predawn plasma trough [*Garrett et al.*, 1981; *Fairfield and Viñas*, 1984; *Sojka and Wrenn*, 1985]. Since no distinction has been made between the "empty" plasma trough and the "refilling" plasma trough as was made by *McComas et al.* [1993], a large percentage of trapped particles, most likely associated with plasma sheet-like particles in the empty plasma trough, and a large percentage of coincident trapped and field-aligned particles, most likely associated with the refilling plasma trough, are both seen in what has simply been termed the plasma trough for this study.

The lack of detectable low-energy electron fluxes in the plasmasphere is most likely due to the fact that plasmaspheric plasma is much cooler than our chosen

Table 2. Percentages of Observations of Each Angular Distribution in the Specific Plasma Regimes

Angular Distribution	Plasma Sheet	Plasma Trough	Plasmasphere
Trapped	31%	63%	6%
Field-aligned	16%	38%	11%
Isotropic	29%	10%	1%
None	28%	17%	84%

low-energy cutoff of 15 eV. The presence of field-aligned fluxes (observed in only 10% of the plasmaspheric encounters) implies that the plasmasphere has not yet reached diffusive equilibrium at which point the electron angular distributions become isotropic [Sojka and Wrenn, 1985].

Much work has recently been done in the area of modeling suprathermal electrons of ionospheric origin and how the dynamics of these particles affects plasmaspheric refilling [Liemohn and Khazanov, 1995; Khazanov et al., 1996]. Typically, these models are initialized with empty plasmaspheric flux tubes, neglecting the presence of low-energy trapped plasma sheet-like electrons in the morning and day sectors. It is not known at this time how the presence of these trapped low-energy electrons may affect the dynamics of field-aligned suprathermal electrons during plasmaspheric refilling.

Acknowledgments. The work at Florida Institute of Technology was partially funded by a NASA SR&T grant (NAGW 5153) and an Associated Western Universities Summer Faculty Fellowship. The work at Los Alamos National Laboratory was done under the auspices of the United States Department of Energy with partial support from NASA's ISTP program.

Janet G. Luhmann thanks Alfred Vampola and another referee for their assistance in evaluating this paper.

References

- Bame, S. J., D. J. McComas, M. F. Thomsen, B. L. Barraclough, R. C. Elphic, J. P. Glore, J. T. Gosling, J. C. Chavez, E. P. Evans, and F. J. Wymer, Magnetospheric plasma analyzer for spacecraft with constrained resources, *Rev. Sci. Instrum.*, **64**, 1026, 1993.
- Carpenter, D. L., Whistler studies of the plasmopause in the magnetosphere, 1, Temporal variations in the position of the knee and some evidence on plasma motions near the knee, *J. Geophys. Res.*, **71**, 693, 1966.
- Chappell, C. R., K. K. Harris, and G. W. Sharp, The morphology of the bulge region of the plasmasphere, *J. Geophys. Res.*, **75**, 3848, 1970.
- Coates, A. J., A. D. Johnstone, J. J. Sojka, and G. L. Wrenn, Ionospheric photoelectrons observed in the magnetosphere at distance up to 7 Earth radii, *Planet. Space Sci.*, **33**, 1267, 1985.
- Cowley, S. W. H., and M. Ashour-Abdalla, Adiabatic plasma convection in a dipole field: Variation of plasma bulk parameters with L , *Planet. Space Sci.*, **23**, 1527, 1975.
- Fairfield, D. H., and A. F. Viñas, The inner edge of the plasma sheet and the diffuse aurora, *J. Geophys. Res.*, **89**, 841, 1984.
- Garrett, H. B., D. C. Schwank, and S. E. DeForest, A statistical analysis of the low energy geosynchronous plasma environment, I, Electrons, *Planet. Space Sci.*, **29**, 1045, 1981.
- Higel, B., and L. Wu, Electron density and plasmopause characteristics at 6.6 R_E : A statistical study of the GEOS 2 relaxation sounder data, *J. Geophys. Res.*, **89**, 1583, 1984.
- Horwitz, J. L., S. Menteer, J. Turnley, J. L. Burch, J. D. Winningham, C. R. Chappell, J. D. Craven, L. A. Frank, and D. W. Slater, Plasma boundaries in the inner magnetosphere, *J. Geophys. Res.*, **91**, 8861, 1986.
- Khazanov, G. V., T. E. Moore, M. W. Liemohn, V. K. Jordanova, and M. C. Fok, Global, collisional model of high energy photoelectrons, *Geophys. Res. Lett.*, **23**, 331, 1996.
- Lee, J. S., J. P. Doering, T. A. Potemra, and L. H. Brace, Measurements of the ambient photoelectron spectrum from Atmospheric Explorer, II, AE-E measurements from 300 to 1000 km during solar minimum conditions, *Planet. Space Sci.*, **28**, 973, 1980.
- Liemohn, M. W., and G. V. Khazanov, Nonsteady state coupling processes in superthermal electron transport, in *Cross-Scale Coupling in Space Plasmas*, *Geophys. Monogr. Ser.*, vol. 93, edited by J. L. Horwitz, N. Singh, and J. L. Burch, p. 181, AGU, Washington, D. C., 1995.
- McComas, D. J., S. J. Bame, B. L. Barraclough, J. R. Donart, R. C. Elphic, J. T. Gosling, M. B. Moldwin, K. R. Moore, and M. F. Thomsen, Magnetospheric plasma analyzer (MPA): Initial three-spacecraft observations from geosynchronous orbit, *J. Geophys. Res.*, **98**, 13453, 1993.
- McIlwain, C. E., and E. C. Whipple, The dynamic behavior of plasmas observed near geosynchronous orbit, *IEEE Trans. Plasma Sci.*, **14**, 874, 1986.
- Moldwin, M. B., M. F. Thomsen, S. J. Bame, D. J. McComas, and K. R. Moore, An examination of the structure and dynamics of the outer plasmopause using multiple geosynchronous satellites, *J. Geophys. Res.*, **100**, 11475, 1994.
- Moldwin, M. B., M. F. Thomsen, S. J. Bame, D. J. McComas, and G. D. Reeves, The fine-scale structure of the outer plasmasphere, *J. Geophys. Res.*, **100**, 8021, 1995.
- Sojka, J. J., and G. L. Wrenn, Refilling of geosynchronous flux tubes as observed at the equator by GEOS 2, *J. Geophys. Res.*, **90**, 6379, 1985.
- Sojka, J. J., R. W. Schunk, J. F. E. Johnson, J. H. Waite, and C. R. Chappell, Characteristics of thermal and suprathermal ions associated with the dayside plasma trough as measured by the Dynamics Explorer retarding ion mass spectrometer, *J. Geophys. Res.*, **88**, 7895, 1983.
- Thomsen, M. F., D. J. McComas, G. D. Reeves, and L. A. Weiss, An observational test of the Tsyganenko (T89a) model of the magnetospheric field, *J. Geophys. Res.*, **101**, 24827, 1996.
- Thomsen, M. F., D. J. McComas, J. E. Borovsky, and R. C. Elphic, The magnetospheric trough, in *Geospace Mass and Energy Flow: Results From the International Solar-Terrestrial Physics Program*, *Geophys. Monogr. Ser.*, vol. 104, edited by J. L. Horwitz, D. L. Gallagher, and W. K. Peterson, p. 355, AGU, Washington, D. C., 1998.
- Vasyliunas, V. M., A survey of low energy electrons in the evening sector of the magnetosphere with OGO 1 and OGO 3, *J. Geophys. Res.*, **73**, 2839, 1968.
- Wrenn, G. L., J. F. E. Johnson, and J. J. Sojka, Stable pancake distributions of low energy electrons in the plasma trough, *Nature*, **279**, 512, 1979.
- Wrenn, G. L., J. J. Sojka, and J. F. E. Johnson, Thermal protons in the morning magnetosphere: Filling and heating near the equatorial plasmopause, *Planet. Space Sci.*, **32**, 351, 1983.
- M. O. Fillingim, Geophysics Program, Box 351650, University of Washington, Seattle WA 98195. (matt@geophys.washington.edu)
- D. J. McComas and M. F. Thomsen, Space and Atmospheric Science Group, Los Alamos National Laboratory, Los Alamos, NM 87545.
- M. B. Moldwin, P. Parrish, and H. K. Rassoul, Department of Physics and Space Sciences, Florida Institute of Technology, Melbourne, FL 32901.

(Received January 29, 1998; revised September 11, 1998; accepted September 11, 1998.)